Direct observation of local hot electron transport through Al2O3 tunnel junctions

DOI:
10.1063/1.1448160

Document status and date:
Published: 01/01/2002

Direct observation of local hot electron transport through Al_2O_3 tunnel junctions

O. Kurnosikov,[a] J. E. A. de Jong, H. J. M. Swagten, and W. J. M. de Jonge
Department of Applied Physics, Eindhoven University of Technology, COBRA Research Institute, P.O. Box 513, 5600 MB, Eindhoven, The Netherlands

(Received 13 September 2001; accepted for publication 30 November 2001)

A modified ballistic electron emission microscopy (BEEM) technique using local transport of hot electrons through a buried interface, was successfully applied to study the Al_2O_3 barrier in the $Co/Al_2O_3/Ru$ tunnel junction. This technique enabled us to straightforwardly measure an effective barrier height of 1.7 eV and to observe the rise of the barrier height due to continuous current injection into a single point of the junction attributed to charging effects and/or degradation of the barrier structure. Scanning over an area of 510 nm×510 nm showed a spatial inhomogenity of the barrier resulting in different dependencies of the BEEM current on the energy of the injected electrons. © *2002 American Institute of Physics.* [DOI: 10.1063/1.1448160]

The recent progress in microelectronic technology is partly based on the application of very thin dielectric films with unique transport properties. In this field, magnetic tunnel junctions (MTJs), consisting of a ferromagnetic–insulator–ferromagnetic thin film trilayer structure, are currently drawing enormous interest. The operation of the MTJs is based on spin-polarized electron transport through the thin insulating layer (often Al_2O_3). Due to the observed large magnetoresistance in MTJs, these structures have great potential for application in digital storage and magnetic sensor devices.

Although a number of nondestructive analytical techniques have provided valuable assets to the characterization of these structures, the *local* structural, electronic, and magnetic properties of the electrodes, the barrier, and the interfaces, are believed to be crucial in understanding the magnetoresistance effect of MTJs. Although common scanning probe techniques, such as atomic force microscopy and scanning tunnel microscopy (STM), do have sufficient spatial resolution, they have insufficient subsurface sensitivity to investigate the properties of the tunnel junction at the barrier or buried interfaces. The so-called ballistic electron emission microscopy (BEEM), based on the STM technique, has the unique ability to measure *subsurface* material properties with high lateral resolution and opens up the possibility of studying MTJs on the local scale using the propagation of hot electrons through a buried interface.

The BEEM method was developed in 1988 by Bell and Kaiser[1] in order to study the quality of Schottky barriers. Later, this method was successfully applied for the analysis of hot electron scattering in thin metallic films deposited on semiconductor substrates.[2] In general, the BEEM method uses a thin film structure with a built-in Schottky barrier several nanometers *below* the surface. Locally injected from an STM tip, the hot electrons are capable of penetrating the bulk of the metal thin film on the depth of the order of a mean free path. Due to the small thickness of the metal overlayer, a non-negligible fraction of these hot electrons can reach the barrier interface ballistically, i.e., without scattering. If the electrons have sufficient energy to overcome the potential barrier, they can be detected in the bottom electrode of the structure as a BEEM current. Varying the energy of injected electrons while scanning the surface, the BEEM current can show a spatial distribution of the transport properties of the barrier.

Recently, the BEEM technique has been expanded to determine the transport properties of Al_2O_3 tunnel barriers.[3,4] However, in these approaches, the Al_2O_3 layer was deposited directly on a semiconductor substrate,[4] or a Schottky barrier was embedded below the tunnel junction[3] in order to decrease the leakage current originating from the nonideal Al_2O_3 barrier. It may be obvious that these Schottky barriers are responsible for additional complexity of the structure and put a limitation on the total thickness of the junction.

In this letter, we show that it is possible to directly measure the transport properties through a tunnel junction by BEEM with a single Al_2O_3 barrier without any auxiliary Schottky barrier. We modified the BEEM technique such that the injected current can be modulated in order to discriminate the BEEM current from a high background leakage current. Using a clean model system of $Co/Al_2O_3/Ru$ as a tunnel junction, we were able to determine the local barrier height and the spatial variation of transmission of the Al_2O_3 barrier. This approach opens up future possibilities of studying complete MTJs with two magnetic electrodes in the presence of external magnetic fields.

Tunnel junction structures of glass/Ta 50 Å/Co 70 Å/Al_2O_3 39–45 Å/Ru 25 Å with junction areas of 300 μm×300 μm were prepared using ultrahigh vacuum (UHV) direct current magnetron sputtering (base pressure $<5\times10^{-10}$ mbar) through shadow masks onto glass substrates; a technique which has been successfully applied before to grow good quality MTJs with magnetoresistance ratios (for $Co/Al_2O_3/Co$ junctions) up to 27% at ~300 K.[5,6] In order to reduce the large background current,

[a]Author to whom correspondence should be addressed; electronic mail: o.kurnosikov@tue.nl

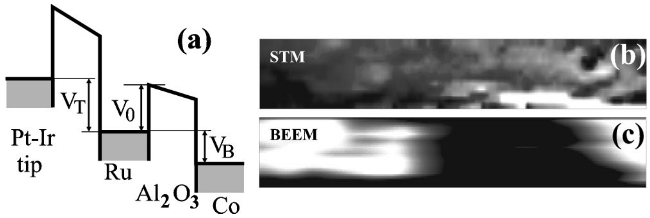

FIG. 1. (a) Energy diagram of the studied system; STM (b) and BEEM (c) images of the junction area of 160 nm×17 nm.

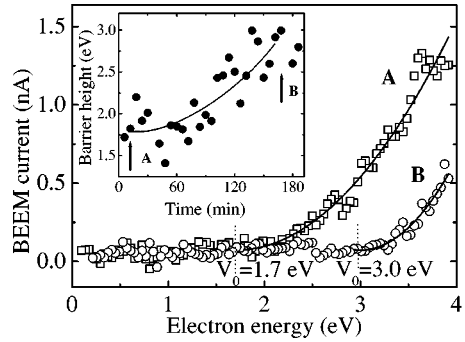

FIG. 2. Dependence of the transparency on the electron energy. (curve A) at the start of the measurement series; (curve B) after 3 h of current injection. Continuous curves represent a fits with power 2 law. The inset represents the evolution of the barrier height in time; the curve in the inset is a guide to the eye only. Arrows A and B mark the points corresponding to the curves A and B.

the tunnel junction was designed for a large resistance ($R > 1.6\times 10^4\ \Omega\,\mathrm{mm}^2$). Completely oxidized Al_2O_3 barriers, thicker than frequently investigated barriers,[7,8] were formed by sufficiently long plasma oxidation of 27–32 Å thick Al layers in 10^{-1} mbar O_2. Second, in order to maximize the BEEM current, a thin overlayer of only 25 Å Ru, which is chemically passive,[9] has been deposited.

BEEM measurements were performed in a home-built air STM/BEEM setup. Ballistic electrons were injected by a Pt–Ir tip at a voltage V_T [see for a diagram Fig. 1(a)]. The charge motion in the barrier towards the collector was improved by applying a bias voltage V_B of 200 mV across the junction. In order to measure the small BEEM current of ballistic electrons on the large background of integral leakage current, a lock-in technique in which the injected current is modulated, was used. The electron energy E was kept constant. A stable alternate injection current I_{STM} with an amplitude of 40 nA $p-p$ and a frequency of 13.78 Hz was achieved by modulating the tip–sample distance under feedback control.

Figures 1(b) and 1(c) show simultaneously taken STM and BEEM pictures of a 160 nm×17 nm area of a Co/Al_2O_3 45 Å/Ru tunnel junction. The STM picture shows a local roughness of approximately 1–2 nm, probably related to the initial roughness of the glass substrate and the poor wetting of metals on Al_2O_3.[6] The BEEM image shows a large variation in detected BEEM current, from 100 pA or less in the black spots to 1.1 nA in the white spots. The lateral dimension of features in the BEEM image is not comparable with the average grain size (10–30 nm), which has been additionally determined by direct STM scanning in air as well as by UHV STM measurements (images are not presented). Furthermore, no correlation at the large scale can be detected between features in the STM and BEEM images, implying that in this case the variations in I_B are independent of the surface structure of the Ru. The variations in I_B are much too large to be associated with a nonuniform distribution of the scattering rate in the Ru overlayer, and must be attributed to variations in the local barrier height V_0, due to, e.g., a nonuniform defect density or thickness variations of the Al_2O_3 layer.

In order to validate these ideas, we studied the dependence of I_B on the energy E of the injected electrons. In Fig. 2, a typical BEEM spectroscopy curve taken at one point on a tunnel junction with a 39 Å thick Al_2O_3 barrier is shown (data set A). Indeed, the current remains negligibly small, until at a specific energy the hot electrons overcome the energy formed by the Al_2O_3 barrier.

This barrier height can be determined by the threshold voltage V_{th} at which the onset in I_B appears. There are several approaches and models to determine V_{th} from experimental data. The simplest assumption of a step-like barrier transmission function $T(E)$ predicts a linear dependence $I_B \propto (V_T - V_0)$.[10] A more advanced model by Bell and Kaiser[1] puts restrictions on the phase space of electrons contributing in I_B, and $I_B \propto (V_T - V_0)^2$. From an improved model by Prietsch,[11] developed for a Schottky barrier and incorporating the energy dependence of $T(E)$ at the interface, it follows $I_B \propto (V_T - V_0)^{5/2}$. Although the experimental results obtained on various Schottky barrier systems can be described by both power 2 and power 5/2 laws, the thresholds resulting from the fits are strongly dependent on the chosen power law.[12]

We applied a power-law transport model of the general form $I_B \propto (V_T - V_0)^n$, where n is an adjustable parameter, to fit data set A, and obtained a best fit around $n=2$ when the mean-square deviation χ^2 is minimal. For this parameter, a local barrier height of 1.7 ± 0.2 eV is derived (Fig. 2).

Using a power 2 law fit on BEEM spectra obtained on complicated Al_2O_3 structures with an additional Schottky barrier, Rippard *et al.* report a barrier height of 1.2 eV for the Al_2O_3 layers of the thickness of about 1 nm.[3] Considering the fact that the Al_2O_3 film in our experiments was 4–5 times thicker, the agreement with our value is reasonable. Ludeke *et al.* have determined a threshold energy of 3.89 eV on a $Si/Al_2O_3/W$ structure with the thickness of the Al_2O_3 layer of about 8 nm, obtained by the atomic layer chemical vapor deposition method.[4] Although there are many reasons to explain the relatively high value of the barrier height in comparison with our and Rippard's[3] results, it can most likely be understood from the structural properties of the Al_2O_3 layer induced by the use of a different growth method directly on the Si substrate. The value of the local barrier height, measured in our experiment, is in better agreement with the integral barrier height of the Al_2O_3 MTJs, which is in the range of 1.8–3.5 eV.[13]

Evolution of the barrier height in time was investigated by measuring 28 spectroscopy curves in a single point during 3 h of current injection (average $I_{inj}=20$ nA). In total, a charge of 2×10^{-4} C has been injected. In Fig. 2(a), spectroscopy curves A and B indicate that V_{th} shifts with more than 1 eV. A tendency of a monotonically increasing barrier height with injection time is observed [see inset of Fig. 2(b)],

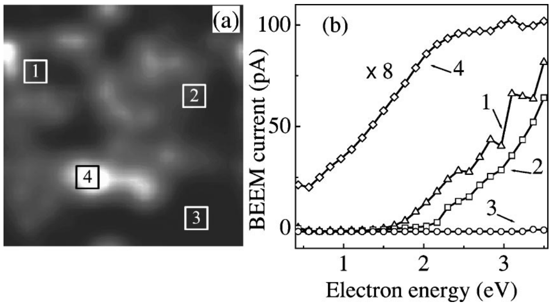

FIG. 3. (a) Spatial variation of transmission of the tunnel junction at 2 eV. Scanning area is 510 nm×510 nm. (b) Spectroscopy curves corresponding to the marked areas of the left panel.

which could be attributed to charging of the barrier, as observed before by Ludeke *et al.*[4,14] During injection, scattered electrons are trapped in existent trapping sites in the bulk Al_2O_3 or in trap states at the barrier interface.[15] However, since the threshold shift appears on a time scale of several hours, the rise in the barrier height could also be explained by degradation of the barrier structure.

The lateral variation of the transport properties of the Co/Al_2O_3 45 Å/Ru tunnel junction was determined by scanning the tip in the range of 510 nm × 510 nm over the Ru surface. In each of the 1600 points covering the scanning area, the spectroscopy curves were measured. Figure 3(a) shows the mapped values of $I_B(E)$ at $E=2$ eV, deduced from each current–voltage ($I-V$) curve. To remove local variations in I_B at neighboring measurement points related to the size of the grains, the data have been smoothed over an area larger than the grain size of the Ru. The BEEM image shows localized features on a scale of 50–100 nm. To further interpret these features, Fig. 3(b) presents the spectroscopy curves 1–4 corresponding to the areas 1–4 marked on Fig. 3(a). The presented curves are the average of the $I-V$ curves measured at 25 neighboring points.

Curves 1 and 2 resemble those presented earlier in Fig. 2, showing the threshold energy for the hot electrons transmitting through the barrier. The deduced barrier heights of 1.5–2.0 eV are in good agreement with the values discussed earlier. The variation in V_0 can be due to lateral variations in the intrinsic barrier properties or from a difference in charging. The absence of a detectable BEEM current in area 3 can be attributed to the local rise of the barrier height above the range of the electron energy used, or to the locally enhanced scattering in the upper metallic layer or at the interface. Area 4 shows a very large transmission in a broad range of electron energies [curve 4 in Fig. 3(b)] and resembles a pinhole. The energy dependence of the transmission at low energies can be interpreted in different ways. In particular, it can originate from the presence of a very low barrier in the pinhole, formed by a defect site of the Al_2O_3, or by CoO. Additionally, a strong $e-e$ scattering, enhancing the number of the hot carriers with low energy at the interface, can be responsible for the significant increase of the current through the pinhole with increasing energy of injected electrons. However, the detailed analysis of the hot electron transport through a pinhole is beyond the scope of the present letter and will be addressed in future studies.

In this letter we have proved that the modified BEEM technique can be applied to nondestructive studies of the barrier properties of the tunnel junctions grown without any auxiliary Schottky barrier. Using this technique, we have found that the height of the Al_2O_3 barrier is about 1.7 eV, however it varies across the junction area as well as in the time due to charging. Additionally, we have found evidence for the energy dependent current transport through a pinhole.

The authors acknowledge P. LeClair and B. Koopmans for valuable discussions and comments. This work forms part of the research program of the Dutch foundation for the Fundamental research on Matter (FOM).

[1] L. D. Bell and W. Kaiser, Phys. Rev. Lett. **61**, 2368 (1988).
[2] R. P. Lu, B. A. Morgan, K. L. Kavanagh, C. J. Powell, P. J. Chen, F. G. Serpa, and W. F. Egelhoff, J. Appl. Phys. **87**, 5164 (2000).
[3] W. H. Rippard, A. C. Perrella, and R. A. Buhrman, Appl. Phys. Lett. **78**, 1601 (2001).
[4] R. Ludeke, M. T. Cuberes, and E. Cartier, Appl. Phys. Lett. **76**, 2886 (2000).
[5] P. LeClair, J. T. Kohlhepp, A. A. Smits, H. J. M. Swagten, B. Koopmans, and W. J. M. de Jonge, J. Appl. Phys. **87**, 6070 (2000).
[6] P. LeClair, H. J. M. Swagten, J. T. Kohlhepp, R. J. M. van de Veerdonk, and W. J. M. de Jonge, Phys. Rev. Lett. **84**, 2933 (2000).
[7] J. S. Moodera, L. R. Kinder, T. M. Wong, and R. Meservey, Phys. Rev. Lett. **74**, 3273 (1995).
[8] J. S. Moodera, L. R. Kinder, J. Nowak, P. LeClair, and R. Meservey, Appl. Phys. Lett. **79**, 708 (1996).
[9] P. Walker and W. H. Tarn, *CRC Handbook of Metal Etching* (Chemical Rubber Corp., Boca Raton, FL, 1991), p. 1415.
[10] H. Palm, M. Arbes, and M. Schulz, Appl. Phys. A: Solids Surf. **56**, 1 (1993).
[11] M. Prietsch, Phys. Rep. **253**, 163 (1995).
[12] M. T. Cuberes, A. Bauer, H. J. Wen, D. Vandre, M. Prietsch, and G. Kaindl, J. Vac. Sci. Technol. B **12**, 2422 (1994).
[13] J. S. Moodera and L. R. Kinder, J. Appl. Phys. **79**, 4724 (1996).
[14] R. Ludeke, M. T. Cuberes, and E. Cartier, J. Vac. Sci. Technol. B **18**, 2153 (2000).
[15] A. Yankova, L. DoThanh, and P. Balk, Solid-State Electron. **30**, 939 (1987).